Received: 14 January 2021 | Revised: 22 July 2021 | Accepted: 27 July 2021

DOI: 10.1111/ddi.13398

METHOD

Diversity and Distributions WILEY

Evaluating models for predicting microclimates across sparsely vegetated and topographically diverse ecosystems

David J. Baker[1,2] | Catherine R. Dickson[2] | Dana M. Bergstrom[3] | Jennie Whinam[4] | Ilya M.D. Maclean[1] | Melodie A. McGeoch[2,5]

[1]Environment and Sustainability Institute, University of Exeter, Penryn, Cornwall, UK

[2]School of Biological Sciences, Monash University, Clayton, Vic., Australia

[3]Australian Antarctic Division, Department of Agriculture, Water and the Environment, Kingston, TAS, Australia

[4]School of Geography and Spatial Science, University of Tasmania, Hobart, TAS, Australia

[5]Department of Ecology, Environment and Evolution, La Trobe University, Melbourne, Vic., Australia

Correspondence
David J. Baker, Environment and Sustainability Institute, University of Exeter, Penryn, Cornwall, UK.
Email: d.baker2@exeter.ac.uk

Funding information
Australian Antarctic Science Program, Grant/Award Number: 4312

Editor: Joern Fischer

Abstract

Aim: Microclimate information is often crucial for understanding ecological patterns and processes, including under climate change, but is typically absent from ecological and biogeographic studies owing to difficulties in obtaining microclimate data. Recent advances in microclimate modelling, however, suggest that microclimate conditions can now be predicted anywhere at any time using hybrid physically and empirically based models. Here, we test these methods across a sparsely vegetated and topographically diverse sub-Antarctic island ecosystem (Macquarie Island).

Innovation: Microclimate predictions were generated at a height of 4 cm above the surface on a 100 × 100 m elevation grid across the island for the snow-free season (Oct–Mar), with models driven by either climate reanalysis data (CRA) or CRA data augmented with meteorological observations from the island's automatic weather station (AWS+CRA). These models were compared with predictions from a simple lapse rate model (LR), where an elevational adjustment was applied to hourly temperature measurements from the AWS. Prediction errors tended to be lower for AWS+CRA-driven models, particularly when compared to the CRA-driven models. The AWS+CRA and LR models had similar prediction errors averaged across the season for T_{min} and T_{mean}, but prediction errors for T_{max} were much smaller for the former. The within-site correlation between observed and predicted daily T_{mean} was on average >0.8 in all months for AWS+CRA predictions and >0.7 in all months for LR predictions, but consistently lower for CRA predictions.

Main conclusions: Prediction of microclimate conditions at ecologically relevant spatial and temporal scales is now possible using hybrid models, and these often provide added value over lapse rate models, particularly for daily extremes and when driven by in situ meteorological observations. These advances will help add the microclimate dimension to ecological and biogeographic studies and aid delivery of climate change-resilient conservation planning in climate change-exposed ecosystems.

KEYWORDS

biogeography, islands, microclima, microrefugia, NicheMapR, polar, threatened ecosystem

1 | INTRODUCTION

Microclimates created by landscape and vegetation structures play a key role in facilitating the persistence of species in locations that would otherwise be climatically inhospitable (Maclean et al., 2015; Suggitt et al., 2018). Without information on microclimates, we observe only course-scale associations between biodiversity and climate, omitting important fine-scale conditions that directly affect organisms (Bütikofer et al., 2020; Storlie et al., 2014), including both horizontal and vertical (i.e. height above or below the surface) variations in climate conditions. Understanding the role of microclimates in structuring biodiversity and facilitating the persistence of species under climate change are vital (Storlie et al., 2014), but studies to date have been limited in geographical and temporal scope by an absence of microclimate data in most locations and for most time periods. However, recent advances in microclimate modelling suggest that microclimate conditions can now be predicted anywhere at any time (Lembrechts & Lenoir, 2020). This claim has profound consequences for biodiversity conservation because climate change is already impacting ecosystems across the globe, and the availability of spatially and temporally explicit microclimate information could help provide a crucial and timely advance in our understanding of how biodiversity is likely to respond.

Because of these data gaps, researchers have been reliant on proxies of microclimate conditions where microclimate variation is thought to be important to the study system. Terrain proxies of microclimate (e.g. slope, aspect, elevation and variables derived from these characteristics, such as wind shelter and topographic wetness indices) have been used frequently in ecological studies, such as for modelling species distributions (Macek et al., 2019) or for evaluating the drivers of ecological processes (Dickson et al., 2019). Terrain proxies essentially assume stationarity in the offset between micro- and macroclimate conditions during the period over which terrain is acting as a proxy; however, this is unlikely during a period of rapid climate change due to changes in weather patterns (Dobrowski, 2011; Maclean et al., 2017). By comparison, the deployment of data loggers is a more direct way to measure fine-scale climate conditions, such as temperature and humidity, and has been used in particular to study the effects of fine-scale temperature and humidity conditions on focal species or ecosystems (Niittynen et al., 2020; Nyakatya & McGeoch, 2008). However, data loggers provide information for point locations only and opportunities for deploying and maintaining microclimate sensor arrays in remote regions are extremely limited. Satellite remote sensing data, by contrast, provide extensive, contiguous spatial coverage of surface temperature conditions—more than 15 years of land surface temperature observations—but with a c. 1-km spatial resolution (e.g. Leihy et al., 2018).

Hybrid physically and empirically based microclimate models offer a computationally efficient and theoretically grounded alternative for obtaining microclimate data across remote regions. These models use well-established physical relationships between near-ground temperatures and a reference air temperature (Maclean et al., 2019) and the modulation of these relationships by landscape physiography (Lembrechts & Lenoir, 2020), to predict hourly temperatures at spatial grains one or two orders of magnitude lower than the best available satellite remote sensing data and at heights above (or below) the surface experienced by organisms. These models provide spatially contiguous fine-scale estimates of biologically important microclimate variation at high temporal resolutions (i.e. hourly). Hybrid models use empirical data (e.g. local meteorological records and digital elevation models) to derive parameter estimates for the physical equations that describe near-surface temperatures at any position in the landscape (Maclean et al., 2017). They predict the microclimate conditions that result from heat exchange at the microclimate scale, as well as mesoclimate effects—such as elevation, cold-air drainage and coastal effects—on the realized microclimate conditions (Maclean et al., 2017). Models are typically parameterized using in situ meteorological observations (e.g. networks of data loggers and meteorological stations), which permit accurate estimation of local conditions (Maclean et al., 2019). The reliance on in situ data has previously been a barrier to microclimate modelling in remote regions. However, with the availability of climate reanalysis data—comprehensive estimates of how weather and climate are changing over time derived from observations and numerical models—which can be used to parameterize microclimate models in these locations, microclimates can now be predicted in any location or time period covered by these data (Lembrechts & Lenoir, 2020).

Robust and comprehensive testing of novel methods is required before they can be used with confidence in ecological and biogeographic studies. Here, we test the ability of a hybrid physically and empirically based microclimate model to reconstruct hourly fine-scale climate conditions (4 cm above the surface on a 100 × 100 m grid) across an exposed, sparsely vegetated, and topographically diverse island ecosystem. Here, microclimate variations generated by topography have been fundamental in structuring the island's unique ecological communities (Ashton & Gill, 1965; Dickson et al., 2021). The models are driven by either (1) hourly air temperature, air pressure, wind speed and direction, and specific humidity measurements from the island's automatic weather station (AWS), augmented by values for atmospheric emissivity, radiation and cloud cover derived from climate reanalysis data products (CRA), or (2) entirely by CRA-derived meteorological variables. The latter aims to test predictions in circumstances where in situ meteorological observations are absent. We benchmark predictions from the hybrid models against predictions from a simple lapse rate model (LR), where an elevational adjustment was applied to hourly temperatures from the AWS. Differences in predictions between models parameterized using AWS data and LR models will be due to processes other than the direct effect of elevation on temperature. These differences help to highlight when and where additional microclimate generating processes are acting. We discuss the game-changing nature of these advances in microclimate modelling for ecological and biogeographical analysis, particularly in remote wilderness locations.

2 | METHODS

2.1 | Study system

Macquarie Island (158°55'E; 54°30'S) is situated in the Southern Ocean. The island covers an area of 128 km^2, is c. 34 km long, is c. 5 km wide and has a maximum elevation of 433 m above sea level (Chown et al., 1998). The island is surrounded by short coastal platforms that rise to steep escarpments (40–80˚), which then graduate to a windswept and treeless alpine plateau undulating between 200 and 433 m above sea level (Selkirk, Seppelt, & Selkirk, 1990). The topographically diverse plateau is interspersed with peaks, rocky scree slopes, creeks, lakes, tarns, and mires across its extent (Selkirk et al., 1990). It is characterized by the sparsely vegetated Macquarie Alpine Mosaic (<50 cm high), and composed of fellfield (<50% cover, also referred to as fjaeldmark and feldmark), open grassland, cushion moorland, open rocky slopes and often linear vegetation terraces, alternating with bare ground, shaped by frost heave (Kitchener & Harris, 2013). The fellfield ecosystem, the major component of the Macquarie Alpine Mosaic, supports a low diversity of both vascular and non-vascular flora, including 18 vascular plant species, 18 mosses, 12 liverworts and 14 lichen species (Selkirk, 2012). The island's climate is cool, misty and windy, with very low daily variations (Dickson et al., 2019; Selkirk et al., 1990). Since 1970, the island's climate has undergone significant changes, including increased precipitation, wind speed and sunshine hours (Adams, 2009; Bergstrom et al., 2015). The island's growing season occurs between October and March during which time the island experiences very little settled snow. This snow-free growing season is the focal time period of this study.

2.2 | Meteorological observations

The Australian Bureau of Meteorology station (#300004) is positioned at the northern isthmus of Macquarie Island (−54.4994 °S 158.9369 °W) at a height of 6 m above sea level. The thermometer and barometer are positioned at a height of 1.2 and 1.3 m above the ground, respectively. Manual records have been collected at the station since 1948 and an automated weather station (AWS) was installed in 1997. At hourly intervals, the AWS records air temperature, dew-point temperature, vapour pressure, wind speed and direction, station-level pressure (later converted to pressure at sea level) and precipitation.

2.3 | Microclimate model

Hourly temperatures were modelled at a height of 4 cm above the ground on a 100 × 100 m resolution grid (from here on 100 m) using the *microclima* (Maclean et al., 2019) and *NicheMapR* (Kearney & Porter, 2017) R packages. In particular, we use the integration of these two packages within the *runauto* function of the *microclima* package (Kearney et al., 2020). This function uses temperatures estimated at each location by *NicheMapR*—mechanistically, using meteorological, elevation and vegetation data as inputs—to calibrate the linear model relating the local temperature anomaly from the reference temperature as a function of net radiation and wind speed (Maclean et al., 2019), as calculated by *microclima*. Without this integration, the *microclima* microclimate model requires in situ mesoclimate and microclimate reference data, collected using an appropriate sampling strategy across the region of interest, to parameterize the model. Microclima is currently unable to account for the effects of soil moisture and snow cover on temperature, which, for the latter in particular, precludes analysis of the winter temperatures on the island.

The hybrid model requires information on location and elevation, sourced automatically or supplied by the user, which, in addition to providing a direct measurement of elevation, is used in connection with landscape information in the calculation of a number of key terrain variables, including the slope and aspect of a cell and terrain shading. These are necessary for calculating the net radiation flux on an inclined surface (Maclean et al., 2019). In this study, a 100 × 100 m digital elevation grid was used, created by aggregating a 5 × 5 m digital elevation model (DEM) of Macquarie Island (Brolsma, 2008) by taking the mean elevation across the finer resolution cells. In the fully automated model, National Centers for Environmental Prediction (NCEP; Kanamitsu et al., 2002; Kemp et al., 2012) climate reanalysis data are downscaled and interpolated to provide hourly information on the reference temperatures and atmospheric forcing conditions that are used to parameterize the model. NCEP (specifically NCEP-DOE reanalysis R-2 [hereafter, NCEP2])-derived variables include temperature at 2 m (°C), specific humidity at 2 m (Kg/Kg), surface pressure (Pa), wind speed at 2 m (m/sec), wind direction (degrees from N), atmospheric emissivity, multiple measures of direct and diffuse radiation, and cloud cover (%). In our analysis, the ground and canopy albedo were fixed across the entire island at 0.15 and 0.23, while *habitat*, which controls how leaf area, leaf geometry and canopy height affect radiation, was specified as “Barren or sparsely vegetated” across the island's extent. For landscapes where shading from vegetation cover is likely to affect the temperatures experienced by organisms, and where the effects of shading vary across the landscape, spatially explicit estimates (i.e. from remote sensing data) of habitat-associated variables can be specified (and similarly for albedo) by supplying spatially explicit values for these parameter. This was not necessary on Macquarie Island given the sparsely distributed and low vegetation structure found across the entire landscape. In these landscapes, terrain is known to have by far the most pronounced effect on microclimate temperature variation (Maclean et al., 2019). Thus, in this analysis, the DEM was the only spatially explicit, user-supplied input to the models.

The hybrid models were driven using either hourly meteorological data obtained from downscaled NCEP2 data (CRA) or using the hourly meteorological observations from the island's AWS for air temperature, air pressure at sea level, wind direction, wind speed and specific humidity, with hourly estimates of the emissivity of the atmosphere, radiation and cloud cover downscaled from NCEP2 data (AWS+CRA; Table 1a). The NCEP2 data (c. 200 × 200 km resolution) were downloaded and temporally interpolated from six-hourly

to hourly values using the hourly NCEP function from *microclima*. An example of how to run the fully automated model can be found in Appendix S1 in the supplementary material. Models were run in hourly time steps for each month across the snow-free period that define the island's growing season (1 October to 30 March).

In addition, we applied a lapse rate model to hourly AWS reference temperatures using the lapse rate function from *microclima*. This function calculates differences in temperature due to elevation as:

$$\Delta T_E = \Delta z \times g \left(1 + \frac{L_v r_v}{QT}\right)\left(c_{pd} + \frac{0.622 L_v^2 r_v}{QT^2}\right)^{-1}$$

where Δz is the elevation difference between a reference location and a second location, g is the gravitation acceleration (9.8076 m/s), L_v is the latent heat of vaporization (2,501,000 J/kg), r_v is the mixing ratio of water vapour, given by $r_v = \frac{0.622 e_a}{P - e_a}$, where P is the atmospheric pressure (Pa) and e_a is the vapour pressure (Pa), Q is the gas constant of dry air (287 J/kg K^{-1}),c_{pd} is the specific heat of dry air at constant pressure (1,003.5 J/kg K^{-1}), and T is the reference air temperature (Maclean et al., 2019).

2.4 | Model evaluation

Model predictions were evaluated against the in situ microclimate observation data (Obs) across the 62 sites (see Table 1b for overview).

TABLE 1 Summary of datasets used in model parameterization and the model evaluation statistics

a)	Microclimate model parameterization data
	1) AWS+CRA (automatic weather station)
	AWS data + NCEP2[a] CRA data
	2) CRA (climate reanalysis)
	NCEP2 CRA data
	3) LR (lapse rate model)
	AWS (air temperature, pressure and humidity) + elevational adjustment
b)	Model evaluation (62 sites)
	Monthly statistics
	(i) Calculate monthly mean of daily $T_{[min, mean, max]}$ for each site for observed and predicted data.
	(ii) Calculate the weighted[b] root mean squared error (RMSE) for observed versus predicted across all 62 evaluation sites.
	Daily statistics
	(i) Calculate the RMSE and Pearson's correlation coefficient (r) for observed versus predicted daily $T_{[min, mean, max]}$ for each site.
	(ii) Calculate weighted[a] mean and standard deviation (*SD*) of RMSE and r across all 62 sites.

[a]National Centers for Environmental Predictions (NCEP)-DOE reanalysis R-2

[b]By number of days of observations per site and month

A stratified random sampling approach was used to select the 62 microclimate monitoring sites across Macquarie Island's plateau ecosystems, stratified by both terrain class and spatial blocks (Dickson et al., 2019). The stratification was designed to maximize the range of microclimate conditions sampled by the data loggers across combinations of latitude, elevation and exposure (i.e. to moisture, wind and solar radiation). We used DS1923 Hygrochron Temperature & Humidity iButtons (Maxim) that were set to record every 4 hr. The data loggers were housed in light grey PVC jars and attached by a free-hanging plastic fob. The jars had three small slats cut into each side to facilitate airflow, while still providing shelter from direct solar radiation and precipitation. The upturned jars and data loggers were attached to stakes 4 cm above the ground, which is representative of the height of most of the plateau vascular and non-vascular flora. Microclimate data loggers were deployed between 16/12/2016 and 28/02/2017 and collected between 25/11/2017 and 03/01/2018 (Table 2; Figure S2.1).

First, because seasonal / monthly averages are often used in ecological studies, we assessed monthly predictions by calculating the weighted root mean squared error (wRMSE) of the monthly average daily T_{min}, T_{mean} and T_{max} between the observed and predicted temperatures across all 62 sites (Table 1b). The wRMSE was calculated as

$$\text{wRMSE} = \sqrt{\frac{\sum_{i=1}^{n} w_i \left(\text{predicted}_i - \text{observed}_i\right)^2}{\sum_{i=1}^{n} w_i}}$$

where w_i is the number of days of observations for each site i per month. Second, we assessed the predictive performance of the models at daily intervals across the complete time series at each site using the RMSE and Pearson's correlation coefficient (r) for each temperature variable (Table 1b); the weighted mean and standard deviation of these within-site RMSE across the 62 sites (see below) are reported, with weights defined as above. We also evaluated the spatial distribution of prediction errors for the daily observed and predicted temperature by mapping the seasonal average predicted minus observed daily T_{min}, T_{mean} and T_{max} for each model type (i.e. AWS, CRA and LR). For all evaluations, the first day and last day of deployment were removed to avoid spurious measurements associated with the installation or removal of the device.

The correlates of daily prediction errors for T_{min}, T_{mean} and T_{max} were assessed using a Bayesian linear model fitted using the brms R package (Bürkner, 2017). We modelled the prediction errors as a function of the distance to the AWS, elevation, aspect, slope and model type. Furthermore, each two-way interaction between model type and each of the four landscape variables was included to test whether the effects of these variables differed between model types. Site was included as a random effect. All variables were standardized prior to model fitting. Models were initial fit assuming a Gaussian distribution for the response variable, but this resulted in models that were underdispersed compared with the observed data. Models were refit assuming a Student distribution for the response and the Gaussian and Student models compared using leave-one-out cross-validation and WAIC. Models assuming a Student distribution

TABLE 2 Weighted root mean squared error (wRMSE) of the monthly mean predictions from microclimate model results against in situ microclimate data loggers. Weights are the number of days of observations per site and month (median and range given for each month)

Month	Number of days of observations (median [min, max])	Weighted root mean squared error (wRMSE) °C								
		AWS+CRA versus Obs			CRA versus Obs			LR versus Obs		
		T_{min}	T_{mean}	T_{max}	T_{min}	T_{mean}	T_{max}	T_{min}	T_{mean}	T_{max}
Oct	31 (31, 31)	**0.45**	0.73	1.02	1.19	1.47	1.91	0.53	**0.38**	**0.78**
Nov	30 (18, 30)	**0.78**	0.57	**0.97**	1.35	1.18	1.76	0.87	**0.47**	1.61
Dec	13 (4, 23)	1.28	**0.52**	1.20	**1.18**	0.64	**1.13**	1.33	0.59	2.75
Jan	24 (3, 31)	**0.73**	**0.49**	1.29	1.00	0.53	**1.03**	0.89	0.64	2.60
Feb	28 (1, 28)	**0.30**	**0.32**	**0.87**	0.88	0.35	1.58	0.49	0.59	2.00
Mar	31 (3, 23)	**0.76**	0.55	0.57	1.23	1.00	1.04	0.83	**0.46**	**0.46**
Mean		**0.72**	0.53	**0.99**	1.14	0.86	1.41	0.82	**0.52**	1.70

The lowest wRMSE for each quantile is highlighted in bold.

Abbreviations: AWS, automated weather station; CRA, climate reanalysis; LR, lapse rate model; Obs, in situ observations.

were preferred in all cases and were able to capture both the mean and the tails of the observed data. As a model selection approach, horseshoe priors were used in order to shrink unimportant parameter estimates towards zero (Carvalho et al., 2010).

Finally, to test the effect of spatial scale on temperature predictions, the two-hybrid models and the lapse rate model were run on a DEM aggregated to a 50 × 50 m (mean elevation). To reduce the computational demands of the finer scale models, the 50-m models were only run for the northern half of the island (north of 54°35'S). Daily T_{min}, T_{mean} and T_{max} predictions are compared for 28 sites based on the two different grid resolutions for each model type (Figure S2.11) and the relationship between the estimates assessed using Pearson's correlation coefficient.

The analysis was conducted using R (version 4.0.1), and the scripts are archived at https://github.com/davidjbaker79/macca_microclimate.

3 | RESULTS

3.1 | Monthly mean statistics

Monthly wRMSE averaged across the snow-free season (Oct to Mar) was consistently lower across all quantiles (T_{min}, T_{mean}, T_{max}) for the hybrid model driven by automatic weather station data (AWS+CRA) than for this same model driven solely by climate reanalysis (CRA) data (Table 2). The hybrid model driven by the AWS+CRA data and the lapse rate (LR) model had similar wRMSE across this same period for T_{min} and T_{mean}, but prediction errors for T_{max} were much lower for the hybrid model (average wRMSE across all months: 0.99 versus 1.70). There was month-to-month variability in model performance (Figure 1), with the monthly T_{mean} predicted with the lowest wRMSE by the AWS+CRA model in three of the months (Oct, Nov and Mar) and by the LR model in the other three months (Dec, Jan and Feb). Monthly mean T_{min} was predicted with the lowest wRMSE in five of the six months by the AWS+CRA model, while prediction errors were much more variable across months for $T_{max,}$ with each model performing best in two of the months (Table 2). There was a consistent pattern of monthly T_{min} values being underestimated (i.e. minimums too warm) across all models, whereas patterns of under- and overestimation were less obvious for the other monthly quantiles (Figure 1). The LR models were not consistently aligned with AWS+CRA predictions, despite both models being driven by the same AWS observation data. This is particularly notable for T_{max}, but can also be seen across other quantiles (Figure 1). The CRA models tend to predict warmer conditions across all quantiles, and in some months show particularly pronounced differences from both the AWS+CRA and LR models, most notably in October and March.

3.2 | Daily statistics

RMSEs for daily T_{min}, T_{mean} and T_{max} were on average lower and less variable across sites for the AWS+CRA model predictions in most months (Figure 2). The across-site mean RMSEs for LR and AWS+CRA predictions were similar, but the across-site variability was generally slightly larger for the LR models, as indicated by the error bars in Figure 2 (showing ±1 *SD*). The across-site mean RMSEs for CRA model predictions were particularly large for T_{min} and were much larger than the AWS+CRA predictions for T_{mean} in some months, but were closer to the AWS+CRA predictions for T_{max}. The within-site correlation between observed and predicted daily T_{mean} was on average >0.8 in all months for AWS+CRA model predictions and >0.7 in all months for LR predictions. Correlation coefficients for daily T_{mean} were on average consistently lower for CRA predictions, but still exceeded 0.6 in all months (Figure 2; Table S2.1; Figure S2.2–2.10). Correlation coefficients for daily T_{min} were typically higher and less variable across sites than those for T_{mean}, while those for T_{max} showed a general decline across most the snow-free season for all models (Figure 2).

Spatial patterns in daily prediction errors averaged across the snow-free season were quite variable across the three models. The

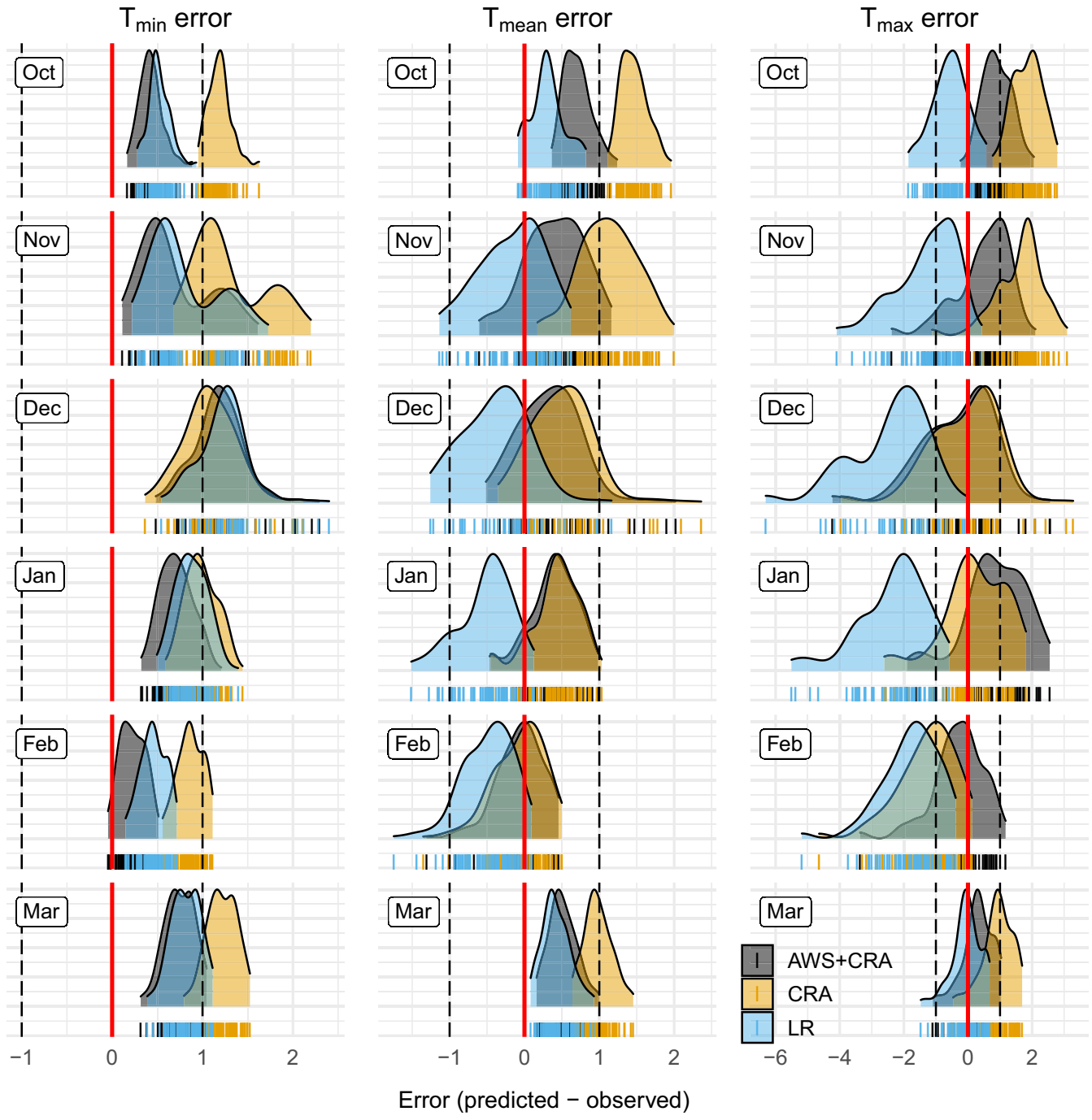

FIGURE 1 Prediction errors (predicted – observed) of the monthly mean predictions from each of the microclimate models and in situ microclimate data loggers (n sites = 62). The tick marks show the errors for each site, and the density of prediction errors is summarized by the density plots. Kernel densities were calculated with weights (n days of observations per site in the month) applied to each observation. Six points from two sites were omitted from the T_{min} panels (three each from Jan and Dec) to aid visualization—these sites had only 4 and 10 days of observation, respectively. AWS =automated weather station; CRA =climate reanalysis; LR =lapse rate model; Obs = in situ observations

CRA model tended on average to overpredicted across all quantiles (Figure 3), while LR models tended to underpredict T_{max} and T_{mean} (predicted < observed), but overpredict T_{min} (predicted > observed). This is consistent with LR models having a smaller diurnal range than observed (mean diurnal range across snow-free season: LR = 3.31°C versus Obs = 4.95°C), while the diurnal range for AWS+CRA and CRA models is closer to the observed (AWS+CRA = 4.89°C; CRA = 4.44°C). The direction of the prediction errors from the AWS+CRA model was less consistent (i.e. to a greater degree distributed around zero), which might suggest less bias towards over- or underpredicting temperatures across the diurnal cycle. There is, however, a tendency for temperatures to be overpredicted in the far south of the island.

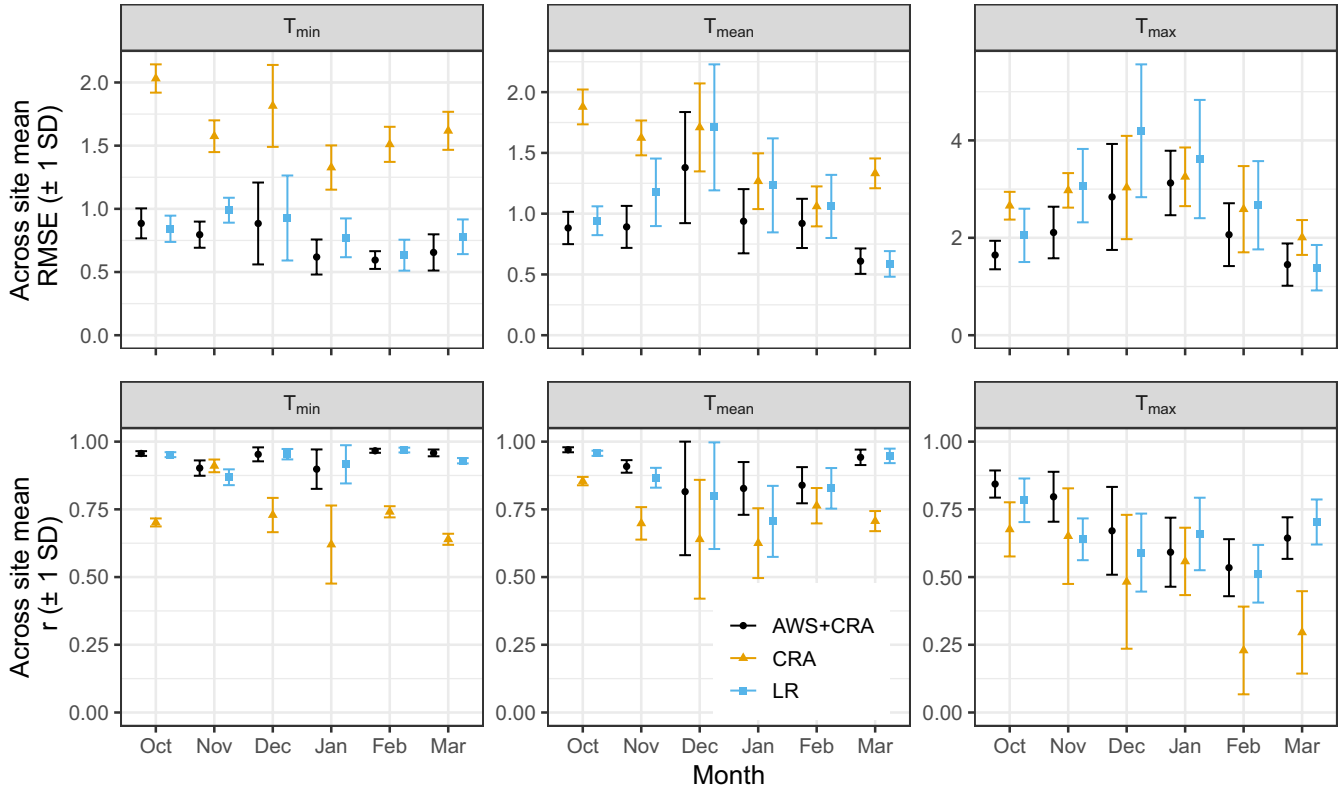

FIGURE 2 Across-site ($n = 62$) weighted mean of within-site root mean squared error (RMSE, ±1 *SD*) and Pearson's correlation coefficient (±1 *SD*) for daily T_{min}, T_{mean}, and T_{max} between each of the microclimate models and in situ microclimate data loggers. AWS =automated weather station; CRA =climate reanalysis; LR =lapse rate model; Obs = in situ observations

3.3 | Correlates of predictions errors

Daily prediction errors were strongly associated with model type across all quantiles, and there is some support for individual positive effects of elevation and aspect on T_{mean} and T_{max} prediction errors. However, there were no significant interactions between landscape variables and model type across each of the quantiles suggesting that errors within models are not consistently associated with particular landscape structures (Figure 4; Table S2.2). Overall, the regression models explained only a small proportion of the variation in the prediction errors [R^2: T_{min} = 0.18 (0.17, 0.19); T_{mean} = 0.11 (0.10, 0.12); T_{max} = 0.10 (0.09, 0.10)].

3.4 | Effects of spatial grain

Predictions of daily T_{min} and T_{mean} between models run at a 100-m and 50-m grain were highly correlated ($r \geq 0.99$) and showed minimal differences (≤0.05°C; Figure S2.11). For T_{max}, the correlation between predictions made at different grain sizes was still high for the AWS+CRA models ($r = 0.97$), but slightly lower for the CRA models ($r = 0.92$). LR models were near perfectly correlated ($r = 1$) across scales, with very low differences in predicted temperatures (<0.001°C).

4 | DISCUSSION

Here, we evaluated the use of a hybrid physically and empirically based modelling approach to predict the daily and seasonal fine-scale climate variation across an exposed, sparsely vegetated, and topographically diverse island ecosystem. Overall, the results show that the hybrid model driven in part by in situ meteorological observations generally provides more accurate estimates of microclimate than a simple elevational lapse rate model, although this was variable month to month and depended on the quantile of interest. The AWS+CRA hybrid models tended to perform better for temperature extremes than the LR model—most notably for predictions of T_{max}—and predict a diurnal range closer to the observed. Temperature extremes, especially maxima, are particularly important for understanding the drivers of species distributions in climatically extreme and variable environments (Easterling et al., 2000) and suggest that simple lapse rate models are not always adequate in such cases. The vegetation across Macquarie Island is reasonably uniform compared with conditions found in even more topographically diverse locations, which means that the lapse rates predictions here, which have error rates for T_{mean} that are comparable to those from the AWS+CRA model, are likely to reflect the best case comparison with the hybrid models. The AWS+CRA model performance was comparable to the performance of mechanistic microclimate models applied to other

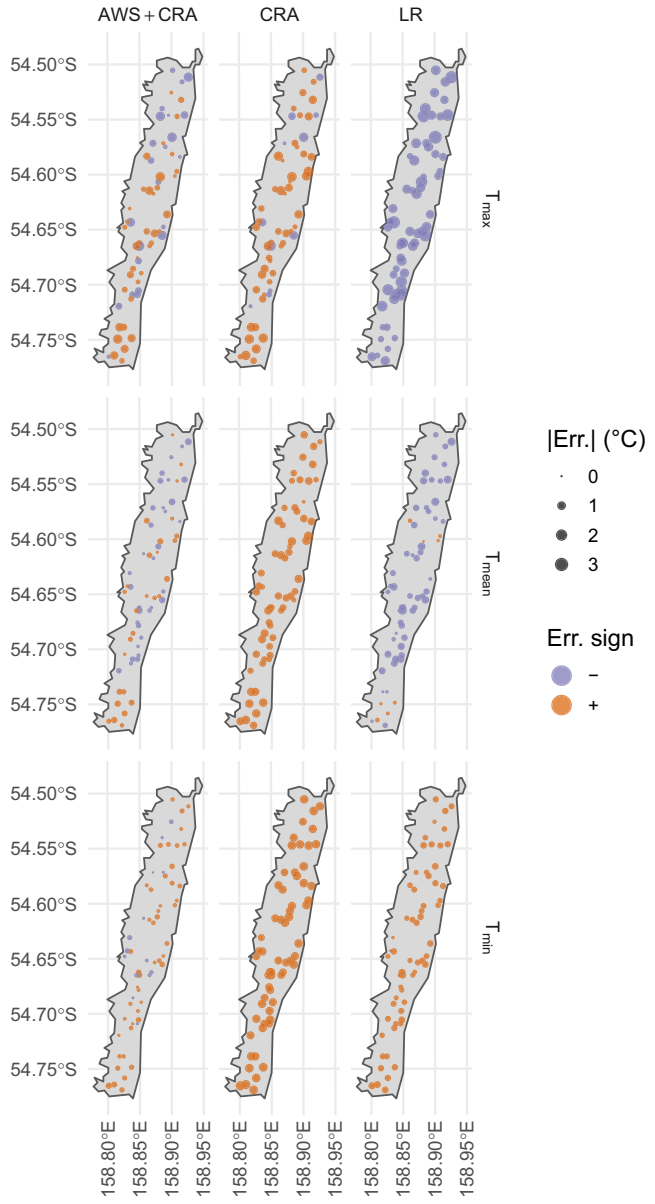

FIGURE 3 The spatial variation in daily prediction error averaged across the snow-free season (Oct–Mar) for T_{min}, T_{mean} and T_{max} across the 62 sites for each of the microclimate models. (-) and (+) indicate an underestimate and an overestimate of the seasonal temperature quantile. Errors are measured in °C (and on a continuous scale). AWS =automated weather station; CRA =climate reanalysis; LR =lapse rate model; Obs = in situ observations

regions, for example a coastal UK peninsula (Kearney et al., 2020; Maclean et al., 2017). The CRA-driven hybrid models, by comparison with the AWS+CRA models, had a warm bias that was evident in most months, but otherwise were able to capture the characteristics (including the diurnal range) of the island's microclimate variation in space and time (Figures S2–10). Therefore, when in situ meteorological observations for a region are not available, microclimate models driven only by climate reanalysis data can be a reasonable alternative to generate predictions of fine-scale climate conditions. Together, our results show that spatially and temporally explicit microclimates can be predicted consistently with low error rates (i.e. monthly means of all quantiles <2°C, and often <1°C) across remote and exposed landmasses, which paves the way for novel and innovative research on the vulnerabilities and conservation opportunities in these challenging and threatened environments.

The models here predicted day-to-day variation in temperature with good accuracy, although there is still error in these predictions and apparent bias in some of the CRA model predictions. The latter is not unexpected as predictions that are unconstrained by in situ data are often biased in some respect, with most climate models (e.g. general circulation models) going through a bias-correction process prior to use (e.g. Navarro-Racines et al., 2020). Some of this error will be caused by differences between the realized macro-, meso- and micro-scale conditions that influence climate variations across a landscape and those captured by the data used to parameterize the models. For example, here we used cloud cover estimates from the NCEP2 reanalysis data, which have a coarse spatial (c. 200 × 200 km) and temporal (6 hr) resolution and, thus, may underestimate variations in cloud cover, especially over a small landmass situated in a vast ocean, or in other locations where cloud cover is heterogeneous. Places with high altitudinal variation on continents may be equally problematic. The reanalysis data may therefore not be entirely representative of the island-specific climatic conditions given the strong maritime influence (Kearney et al., 2020), and this suggests that model performance might improve further if driven by reanalysis data run at higher spatial and temporal resolutions (e.g. Posselt et al., 2012). Similarly, the summary of digital elevation information from a fine grain (i.e. 5 × 5 m) to the grain at which the model is run (100 × 100 m) will introduce variation into the model predictions, although these scale effects do not appear to be strong in this landscape (see Figure S2.11). The effects of these choices will vary across different landscapes depending on the spatial scales over which topographic variation affects microclimates. The optimal spatial scales at which to predict microclimate will be system-specific (Bütikofer et al., 2020), and there is likely to be trade-off between spatial grain and uncertainty in the elevation data and from other model parameters (e.g. vegetation type, height and cover). Previous studies have shown that the main differences in microclimate conditions occur between grains >1 km and 100 m (Gillingham et al., 2012).

There will also always be some measurement errors from the iButton temperature loggers, which can be large under certain conditions (Maclean et al., 2021), and this may reduce the accuracy of the benchmark against which to compare the models. These effects might be minimized on Macquarie island due to the consistent sub-Antarctic winds blowing at high speed across the island, which produces strong thermal mixing of the air, the high cloud cover, which reduces the expose of the shielded sensor to solar radiation, and the low surface albedo. Measurements of T_{max} are the most likely to be affected (e.g. temperature spikes during by sunny, still spells), although here T_{max} was most likely to be overestimated by the hybrid models, suggesting that these errors are not likely to be common in this system. Nevertheless, there is an urgent need to prioritize the

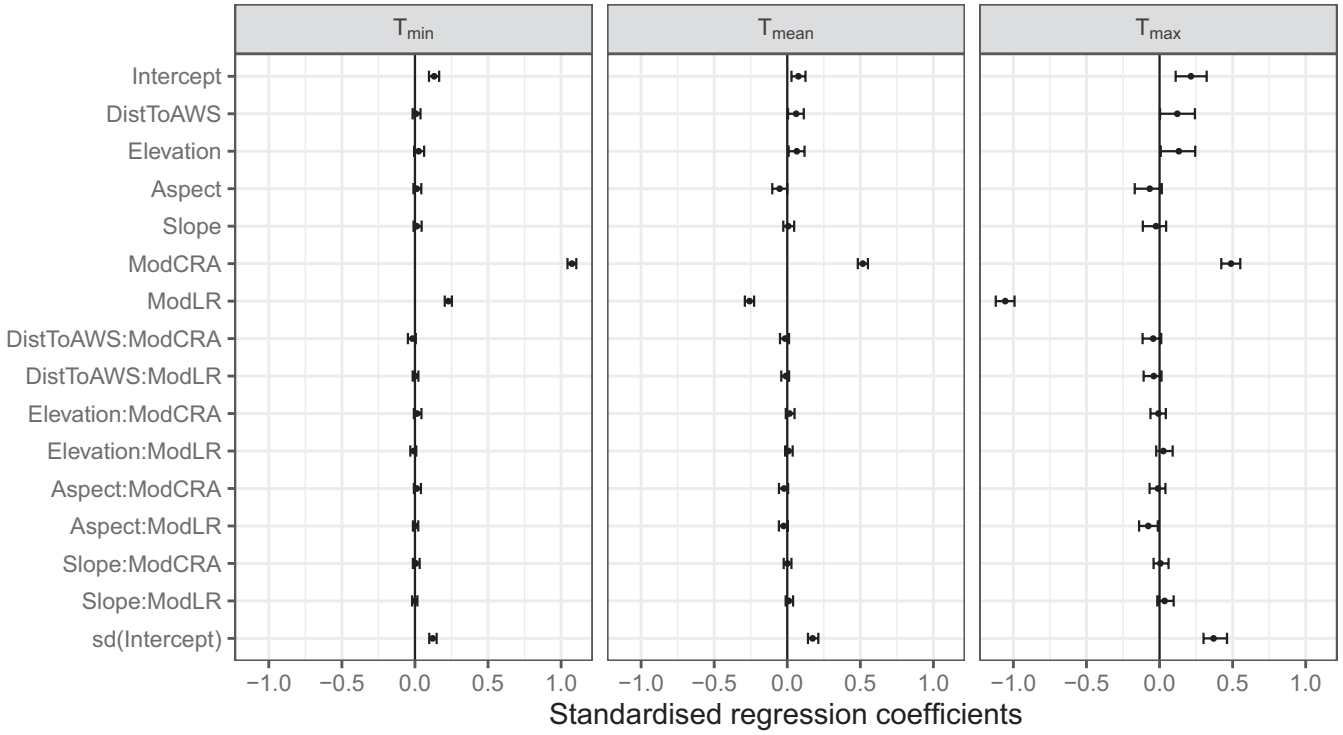

FIGURE 4 Standardized regression coefficients for linear models estimating the effect of microclimate model type, landscape variables, and their interactions on prediction errors for daily T_{min}, T_{mean} and T_{max}. Estimates are shown as median (l-95% CI, u-95% CI)

collection of microclimate measurements using the most state-of-the-art instruments in a range of environments in order to further enhance our understanding of where we are best able to predict microclimate conditions and where further refinement of models and methods are required.

The results here show that the hybrid physically and empirically based modelling approach, and in particular the AWS+CRA-driven model, can routinely provide predictions of seasonal temperature variation and averages with error rates of <2°C across all quantiles, and typically <1°C for the AWS+CRA models (Table 2). The monthly wRMSE for the AWS+CRA model compares favourably with Ashcroft et al. (2009) predictions of spatially contiguous seasonal climate grids produced with a correlative approach, which ranged from 0.5 to 3.4°C depending on the quantile being evaluated. The difference here is that the model does not require the deployment of hundreds of temperature data loggers for the calibration and model fitting, only data from a single observation station. Also, because the model is not reliant on in situ data logger data for calibration, we can predict microclimates for time periods when in situ microclimate sensor data are not available. The RMSE produced here was smaller than RMSE of satellite remote sensing (c. 1-km grain) tested on Marion Island in the Southern Ocean (Leihy et al., 2018), although the difference in grain size (100 m versus 1 km) makes a direct comparison difficult. Thus, the hybrid physically and empirically based modelling approach appears to offer performance and logistical advantages over other commonly used methods used to obtain microclimate data. These logistical advantages are important because microclimate data are urgently needed to underpin fundamental and applied ecological research across the breadth of terrestrial ecosystems and species groups (e.g. Jucker et al., 2020; Nowakowski et al., 2018). In particular, conservation strategies centred around identifying potential microrefugia have received much interest, especially for species that cannot track shifting climate niches or adapt in situ to changing climate conditions (Ashcroft, 2010; Wilson et al., 2019). Importantly, by understanding the role of microclimates in structuring biodiversity—for example through effects on species physiology, demography and behaviour—it may also be possible to modify landscapes to increase their climate change resilience (Jucker et al., 2020; Shoo et al., 2011). These research questions are most pressing given the stress that climate change is already placing on biodiversity (Descamps et al., 2017). Thus, the capability of predicting spatially and temporally contiguous microclimates with low error rates at scales relevant to a focal system or species is the most significant outcome of these technical advances because microclimate datasets can now be rapidly produced for locations and time period that correspond to existing ecological dataset, where contemporaneous in situ microclimate measurements are not available (Lembrechts & Lenoir, 2020).

Physically and empirically based microclimate models show considerable promise for predicting ecologically meaningful microclimate conditions across climate change-vulnerable ecosystems, particularly when in situ meteorological data are available, but also in locations and for time periods where these data are absent but where climate reanalysis data are available. This paves the way for novel ecological and biogeographic studies on the role of microclimate in determining biodiversity patterns and trends. Projections

of future changes in microclimate conditions are also possible (i.e. Maclean, 2020), and these will be invaluable for understanding the plausible range of changes in microclimate conditions across the region and for predicting the threats that these changes pose to biodiversity (e.g. Lembrechts et al., 2019). These advances in estimating microclimates stand to significantly improve climate change-resilient conservation planning.

ACKNOWLEDGEMENTS

We thank Aleks Terauds, Ben Raymond and Justine Shaw for discussion and logistical advice. Kate Kiefer provided logistical and field support. John Burgess, Rowena Hannaford and the 69th and 70th Macquarie Island Australian Antarctic Program teams helped establish and retrieve the data loggers. We are grateful to the editor and two anonymous reviewers for comments on an earlier version of this work. This research was funded by the Australian Antarctic Division and the Australian Government under an Australian Antarctic Science Program Grant #4312, and support to CRD from an Australian Government Research Training Program (RTP) Scholarship.

CONFLICTS OF INTEREST

The authors declare no conflicts of interest.

PEER REVIEW

The peer review history for this article is available at https://publons.com/publon/10.1111/ddi.13398.

DATA AVAILABILITY STATEMENT

The iButton microclimate data are publicly archived at https://data.aad.gov.au/metadata/records/AAS_4312_MI_microclimate_data_Dec16Dec17_62sites, and Macquarie Island automatic weather station data can be downloaded from https://data.aad.gov.au/aws/.

ORCID

David J. Baker https://orcid.org/0000-0002-0466-8222
Ilya M.D. Maclean https://orcid.org/0000-0001-8030-9136
Melodie A. McGeoch https://orcid.org/0000-0003-3388-2241

REFERENCES

Adams, N. (2009). Climate trends at Macquarie Island and expectations of future climate change in the sub-Antarctic. *Papers and Proceedings of the Royal Society of Tasmania*, *143*(1), 1–8. https://doi.org/10.26749/rstpp.143.1.1

Ashcroft, M. B. (2010). Identifying refugia from climate change. *Journal of Biogeography*, *37*(8), 1407–1413. https://doi.org/10.1111/j.1365-2699.2010.02300.x

Ashcroft, M. B., Chisholm, L. A., & French, K. O. (2009). Climate change at the landscape scale: Predicting fine-grained spatial heterogeneity in warming and potential refugia for vegetation. *Global Change Biology*, *15*(3), 656–667. https://doi.org/10.1111/j.1365-2486.2008.01762.x

Ashton, D. H., & Gill, A. M. (1965). Pattern and process in a Macquarie Island feldmark. *Proceedings of the Royal Society of Victoria*, *79*, 235–245.

Bergstrom, D. M., Bricher, P. K., Raymond, B., Terauds, A., Doley, D., McGeoch, M. A., Whinam, J., Glen, M., Yuan, Z., Kiefer, K., Shaw, J. D., Bramely-Alves, J., Rudman, T., Mohammed, C., Lucieer, A., Visoiu, M., Jansen van Vuuren, B., & Ball, M. C. (2015). Rapid collapse of a sub-Antarctic alpine ecosystem: The role of climate and pathogens. *Journal of Applied Ecology*, *52*(3), 774–783. https://doi.org/10.1111/1365-2664.12436

Brolsma, H. (2008). Macquarie Island AIRSAR DEM (Digital Elevation Model). http://data.aad.gov.au/aadc/metadata/.

Bürkner, P. C. (2017). brms: An R package for Bayesian multilevel models using Stan. *Journal of Statistical Software*, *80*(Plummer 2013). https://doi.org/10.18637/jss.v080.i01

Bütikofer, L., Anderson, K., Bebber, D. P., Bennie, J. J., Early, R. I., & Maclean, I. M. D. (2020). The problem of scale in predicting biological responses to climate. *Global Change Biology*, *26*(12), 6657–6666. https://doi.org/10.1111/gcb.15358

Carvalho, C. M., Polson, N. G., & Scott, J. G. (2010). The horseshoe estimator for sparse signals. *Biometrika*, *97*(2), 465–480. https://doi.org/10.1093/biomet/asq017

Chown, S. L., Gremmen, N. J. M., & Gaston, K. J. (1998). Ecological biogeography of southern Ocean Islands: Species-area relationships, human impacts, and conservation. *The American Naturalist*, *152*(4), 562–575. https://doi.org/10.1086/286190

Descamps, S., Aars, J., Fuglei, E., Kovacs, K. M., Lydersen, C., Pavlova, O., Pedersen, Å. Ø., Ravolainen, V., & Strøm, H. (2017). Climate change impacts on wildlife in a High Arctic archipelago – Svalbard. Norway. *Global Change Biology*, *23*(2), 490–502. https://doi.org/10.1111/gcb.13381

Dickson, C. R., Baker, D. J., Bergstrom, D. M., Bricher, P. K., Brookes, R. H., Raymond, B., Selkirk, P. M., Shaw, J. D., Terauds, A., Whinam, J., & McGeoch, M. A. (2019). Spatial variation in the ongoing and widespread decline of a keystone plant species. *Austral Ecology*, *44*, 891–905. https://doi.org/10.1111/aec.12758

Dickson, C. R., Baker, D. J., Bergstrom, D. M., Brookes, R. H., Whinam, J., & McGeoch, M. A. (2021). Widespread dieback in a foundation species on a sub-Antarctic World Heritage Island: Fine-scale patterns and likely drivers. *Austral Ecology*, *46*(1), 52–64. https://doi.org/10.1111/aec.12958

Dobrowski, S. Z. (2011). A climatic basis for microrefugia: The influence of terrain on climate. *Global Change Biology*, *17*(2), 1022–1035. https://doi.org/10.1111/j.1365-2486.2010.02263.x

Easterling, D. R., Meehl, G. A., Parmesan, C., Changnon, S. A., Karl, T. R., & Mearns, L. O. (2000). Climate extremes: observations, modeling, and impacts. *Science*, *289*(5487), 2068–2074

Gillingham, P. K., Huntley, B., Kunin, W. E., & Thomas, C. D. (2012). The effect of spatial resolution on projected responses to climate warming. *Diversity and Distributions*, *18*, 990–1000. https://doi.org/10.1111/j.1472-4642.2012.00933.x

Jucker, T., Jackson, T. D., Zellweger, F., Swinfield, T., Gregory, N., Williamson, J., Slade, E. M., Phillips, J. W., Bittencourt, P. R. L., Blonder, B., Boyle, M. J. W., Ellwood, M. D. F., Hemprich-Bennett, D., Lewis, O. T., Matula, R., Senior, R. A., Shenkin, A., Svátek, M., & Coomes, D. A. (2020). A Research Agenda for microclimate ecology in human-modified tropical forests. *Frontiers in Forests and Global Change*, *2*(January), 1–11. https://doi.org/10.3389/ffgc.2019.00092

Kanamitsu, M., Ebisuzaki, W., Woollen, J., Yang, S.-K., Hnilo, J. J., Fiorino, M., & Potter, G. L. (2002). NCEP-DOE AMIP-II Reanalysis (R-2). *Bulletin of the American Meteorological Society*, *83*(11), 1631–1644. https://doi.org/10.1175/BAMS-83-11-1631

Kearney, M. R., Gillingham, P. K., Bramer, I., Duffy, J. P., & Maclean, I. M. D. (2020). A method for computing hourly, historical, terrain-corrected microclimate anywhere on earth. *Methods in Ecology and Evolution*, *11*(1), 38–43. https://doi.org/10.1111/2041-210X.13330

Kearney, M. R., & Porter, W. P. (2017). NicheMapR – an R package for biophysical modelling: The microclimate model. *Ecography*, *40*(5), 664–674. https://doi.org/10.1111/ecog.02360

Kemp, M. U., Emiel van Loon, E., Shamoun-Baranes, J., & Bouten, W. (2012). RNCEP: Global weather and climate data at your

fingertips. *Methods in Ecology and Evolution*, *3*(1), 65–70. https://doi.org/10.1111/j.2041-210X.2011.00138.x

Kitchener, A., & Harris, S. (2013). *From Forest to Fjaeldmark: Descriptions of Tasmania's Vegetation*, 2nd ed. Department of Primary Industries, Parks, Water and Environment.

Leihy, R. I., Duffy, G. A., Nortje, E., & Chown, S. L. (2018). Data descriptor: High resolution temperature data for ecological research and management on the Southern Ocean Islands. *Scientific Data*, *5*, 180177. https://doi.org/10.1038/sdata.2018.177

Lembrechts, J. J., & Lenoir, J. (2020). Microclimatic conditions anywhere at any time! *Global Change Biology*, *26*(2), 337–339. https://doi.org/10.1111/gcb.14942

Lembrechts, J. J., Nijs, I., & Lenoir, J. (2019). Incorporating microclimate into species distribution models. *Ecography*, *42*(7), 1267–1279. https://doi.org/10.1111/ecog.03947

Macek, M., Kopecký, M., & Wild, J. (2019). Maximum air temperature controlled by landscape topography affects plant species composition in temperate forests. *Landscape Ecology*, *34*(11), 2541–2556. https://doi.org/10.1007/s10980-019-00903-x

Maclean, I. M. D. (2020). Predicting future climate at high spatial and temporal resolution. *Global Change Biology*, *26*(2), 1003–1011. https://doi.org/10.1111/gcb.14876

Maclean, I. M. D., Duffy, J. P., Haesen, S., Govaert, S., Frenne, P. De, Vanneste, T., Meerbeek, K.V. (2021). On the measurement of microclimate. *Methods in Ecology and Evolution*, *12*(8), 1397–1410. https://doi.org/10.1111/2041-210X.13627

Maclean, I. M. D., Hopkins, J. J., Bennie, J., Lawson, C. R., & Wilson, R. J. (2015). Microclimates buffer the responses of plant communities to climate change. *Global Ecology and Biogeography*, *24*(11), 1340–1350. https://doi.org/10.1111/geb.12359

Maclean, I. M. D., Mosedale, J. R., & Bennie, J. J. (2019). Microclima: An r package for modelling meso- and microclimate. *Methods in Ecology and Evolution*, *10*(2), 280–290. https://doi.org/10.1111/2041-210X.13093

Maclean, I. M. D., Suggitt, A. J., Wilson, R. J., Duffy, J. P., & Bennie, J. J. (2017). Fine-scale climate change: Modelling spatial variation in biologically meaningful rates of warming. *Global Change Biology*, *23*(1), 256–268. https://doi.org/10.1111/gcb.13343

Navarro-Racines, C., Tarapues, J., Thornton, P., Jarvis, A., & Ramirez-Villegas, J. (2020). High-resolution and bias-corrected CMIP5 projections for climate change impact assessments. *Scientific Data*, *7*(1), 7. https://doi.org/10.1038/s41597-019-0343-8

Niittynen, P., Heikkinen, R. K., Aalto, J., Guisan, A., Kemppinen, J., & Luoto, M. (2020). Fine-scale tundra vegetation patterns are strongly related to winter thermal conditions. *Nature Climate Change*, *10*(12), 1143–1148. https://doi.org/10.1038/s41558-020-00916-4

Nowakowski, A. J., Frishkoff, L. O., Agha, M., Todd, B. D., & Scheffers, B. R. (2018). Changing thermal landscapes: merging climate science and landscape ecology through thermal biology. *Current Landscape Ecology Reports*, *3*(4), 57–72. https://doi.org/10.1007/s40823-018-0034-8

Nyakatya, M. J., & McGeoch, M. A. (2008). Temperature variation across Marion Island associated with a keystone plant species (Azorella selago Hook. (Apiaceae)). *Polar Biology*, *31*(2), 139–151. https://doi.org/10.1007/s00300-007-0341-8

Posselt, R., Mueller, R. W., Stöckli, R., & Trentmann, J. (2012). Remote Sensing of Environment Remote sensing of solar surface radiation for climate monitoring — the CM-SAF retrieval in international comparison. *Remote Sensing of Environment*, *118*, 186–198. https://doi.org/10.1016/j.rse.2011.11.016

Selkirk, P. M. (2012). Plateau vegetation on Sub-Antarctic Macquarie Island. *Papers and Proceedings of the Royal Society of Tasmania*, *146*(1894), 71–79.

Selkirk, P. M., Seppelt, R. D., & Selkirk, D. R. (1990). *Subantarctic Macquarie Island: environment and biology*. Cambridge Press University Press.

Shoo, L. P., Olson, D. H., McMenamin, S. K., Murray, K. A., Van Sluys, M., Donnelly, M. A., Stratford, D., Terhivuo, J., Merino-Viteri, A., Herbert, S. M., Bishop, P. J., Corn, P. S., Dovey, L., Griffiths, R. A., Lowe, K., Mahony, M., McCallum, H., Shuker, J. D., Simpkins, C., … Hero, J.-M. (2011). Engineering a future for amphibians under climate change. *Journal of Applied Ecology*, *48*(2), 487–492. https://doi.org/10.1111/j.1365-2664.2010.01942.x

Storlie, C., Merino-Viteri, A., Phillips, B., VanDerWal, J., Welbergen, J., & Williams, S. (2014). Stepping inside the niche: Microclimate data are critical for accurate assessment of species' vulnerability to climate change. *Biology Letters*, *10*(9), 20140576. https://doi.org/10.1098/rsbl.2014.0576

Suggitt, A. J., Wilson, R. J., Isaac, N. J. B., Beale, C. M., Auffret, A. G., August, T., Bennie, J. J., Crick, H. Q. P., Duffield, S., Fox, R., Hopkins, J. J., Macgregor, N. A., Morecroft, M. D., Walker, K. J., & Maclean, I. M. D. (2018). Extinction risk from climate change is reduced by microclimatic buffering. *Nature Climate Change*, *8*(8), 713–717. https://doi.org/10.1038/s41558-018-0231-9

Wilson, O. J., Walters, R. J., Mayle, F. E., Lingner, D. V., & Vibrans, A. C. (2019). Cold spot microrefugia hold the key to survival for Brazil's Critically Endangered Araucaria tree. *Global Change Biology*, *25*(12), 4339–4351. https://doi.org/10.1111/gcb.14755

BIOSKETCH

The authors are ecologists and biogeographers interested in developing insights into the effects of climate change on biodiversity, with a particular aim of informing conservation planning in some of the most climate change-threatened ecosystems.

SUPPORTING INFORMATION

Additional supporting information may be found online in the Supporting Information section.

How to cite this article: Baker, D. J., Dickson, C. R., Bergstrom, D. M., Whinam, J., Maclean, I. M. D., & McGeoch, M. A. (2021). Evaluating models for predicting microclimates across sparsely vegetated and topographically diverse ecosystems. *Diversity and Distributions*, 27, 2093–2103. https://doi.org/10.1111/ddi.13398